AFCRL-71-0500

013630-8-T

THE UNIVERSITY OF MICHIGAN

COLLEGE OF ENGINEERING
DEPARTMENT OF ELECTRICAL ENGINEERING
Radiation Laboratory

Techniques for Broadband Control of Radar Cross Sections

By
VALDIS V. LIEPA and E. LAWRENCE McMAHON

September 1971

Scientific Report No. 11
Contract No. F19628-68-C-0071
Project No. 5635
Task No. 563502
Work Unit No. 56350201

Approved for public release; distribution unlimited.

Contract Monitor: JOHN K. SCHINDLER
MICROWAVE PHYSICS LABORATORY

Prepared for:

Air Force Cambridge Research Laboratories
Air Force Systems Command
Laurence G. Hanscom Field
Bedford, Massachusetts 01730

Administered through:

OFFICE OF RESEARCH ADMINISTRATION • ANN ARBOR

UNCLASSIFIED

Security Classification

DOCUMENT CONTROL DATA - R & D

(Security classification of title, body of abstract and indexing annotation must be entered when the overall report is classified)

1. ORIGINATING ACTIVITY (Corporate author)	2a. REPORT SECURITY CLASSIFICATION
The University of Michigan, Radiation Laboratory Department of Electrical and Computer Engineering 2455 Hayward Street, Ann Arbor, Michigan 48105	UNCLASSIFIED 2b. GROUP ------

3. REPORT TITLE

TECHNIQUES FOR BROADBAND CONTROL OF RADAR CROSS SECTIONS

4. DESCRIPTIVE NOTES (Type of report and inclusive dates)

Scientific Interim

5. AUTHOR(S) (First name, middle initial, last name)

Valdis V. Liepa
E. Lawrence McMahon

6. REPORT DATE	7a. TOTAL NO. OF PAGES	7b. NO OF REFS
September 1971	49	20

8a. CONTRACT OR GRANT NO.	9a. ORIGINATOR'S REPORT NUMBER(S)
F19628-68-C-0071	013630-8-T
b. PROJECT NO Project, Task, Work Unit Nos. 5635-02-01 DoD Element 61102F	Scientific Report No. 11
c. DoD Subelement 681305	9b. OTHER REPORT NO(S) (Any other numbers that may be assigned this report) AFCRL-71-0500

10. DISTRIBUTION STATEMENT

A -- Approved for public release; distribution unlimited.

11. SUPPLEMENTARY NOTES	12. SPONSORING MILITARY ACTIVITY
TECH, OTHER	Air Force Cambridge Research Laboratories (LZ) L. G. Hanscom Field Bedford, Massachusetts 01730

13. ABSTRACT

Methods of realizing the load impedance required for radar cross section control of conducting bodies are discussed. It is shown that passive loading, using frequency-dependent dielectric/magnetic materials in a radial or coaxial line, requires a frequency dependence which is not exhibited by any known material.

A number of active synthesis approaches are examined, with emphasis on those using the Negative Impedance Converter (NIC). Experimental results are given for a particular NIC realization operating in the 5 - 10 MHz range; the circuit is shown to be capable of producing the load impedance required for a cross-section reduction of 13dB or more over a 2:1 bandwidth.

DD FORM 1 NOV 1473

UNCLASSIFIED

Security Classification

KEY WORDS	LINK A		LINK B		LINK C	
	ROLE	WT	ROLE	WT	ROLE	WT
Impedance Loading						
Active Synthesis						
Negative Impedance Converter						
Broadband						
Reduction of Back Scattering						
Radar Cross Section Control						

Techniques for Broadband Control of Radar Cross Sections

By

Valdis V. Liepa and E. Lawrence McMahon
The University of Michigan
Radiation Laboratory
2455 Hayward Street
Ann Arbor, Michigan 48105

September 1971

Scientific Report No. 11
Contract F19628-68-C-0071
Project No. 5635
Task No. 563502
Work Unit No. 56350201

Approved for public release; distribution unlimited.

Contract Monitor: John K. Schindler
Microwave Physics Laboratory

Prepared For

Air Force Cambridge Research Laboratories
Air Force Systems Command
Laurence G. Hanscom Field
Bedford, Massachusetts 01730

ABSTRACT

Methods of realizing the load impedance required for radar cross section control of conducting bodies are discussed. It is shown that passive loading, using frequency-dependent dielectric/magnetic materials in a radial or coaxial line, requires a frequency dependence which is not exhibited by any known material.

A number of active synthesis approaches are examined, with emphasis on those using the Negative Impedance Converter (NIC). Experimental results are given for a particular NIC realization operating in the 5 - 10 MHz range; the circuit is shown to be capable of producing the load impedance required for a cross-section reduction of 13dB or more over a 2:1 bandwidth.

TABLE OF CONTENTS

ACKNOWLEDGEMENTS

The authors wish to express their gratitude to Prof. T.B.A. Senior, who directed and coordinated the work described in this report, and who also contributed a great deal through discussions, comments, etc. Our special thanks are due to Mr. Charles B. Loftis, who performed most of the tedious experimental work and many of the calculations; his contributions to the experimental work were invaluable.

I

INTRODUCTION

Impedance (or reactive) loading is a potentially powerful method for modifying scattering behavior and. in particular, for reducing the back scattering cross section of an object.

Theoretically at least, it is possible to modify the scattering in almost any desired manner providing the loading configuration has the required sophistication; in particular, zero back scattering is feasible. Not surprisingly, the exact loading necessary to achieve this depends on the shape and size of the target, the location of the load and, in general, the direction of the incidence. It is also a critical function of frequency, which is the principal drawback, but in spite of this, the method has been shown to work over a few per cent bandwidth for a variety of simple target shapes including spheres, cylinders (thick and thin), and spheroids.

In essence, the technique is to introduce an impedance over a restricted portion of the surface using a cavity-backed slot, lumped network or other type of microwave circuit, and as such it is only a special case of the general theory of surface impedance effects. Mathematically at least, it is similar to the application of absorbers, but in practice differs both in the localized nature of the region where the loading is employed and in the greater variety of impedances that can be achieved either to enhance or decrease the scattered field. Alternatively, one could seek to generate the loading by attaching dipoles or other stub antennas to the surface of the target, and this technique has also received some attention. In either case, the present limitations of the loading method remain the same, namely, sensitivity to frequency and aspect.

Whether the loading to provide the desired radar cross section control is provided by cutting slots in the surface or by attaching external scatterers, the frequency behavior of the impedances associated with these loading devices is

(at least qualitatively) independent of the shape of the body and the position of the load, and is the opposite of that provided by a series RLC network or shorted transmission line. Consequently, when such means are used to simulate the desired loading, the exact impedance can be provided only at a single frequency, which then leads to a narrow-band performance.

Over the last few years the Radiation Laboratory has sought ways of increasing the bandwidth of the impedance loading technique with particular reference to the frequency range 50-100 MHz. Both active and passive methods of realizing the required loads have been studied and we here present some of the results obtained. Section II summarizes some of our earlier theoretical and experimental work on the loading method and, in particular, shows the type of loading variation with frequency necessary to suppress back scattering cross sections in the resonance region. The possibility of achieving this variation by inserting a frequency-dependent material into a radial cavity or coaxial line is examined in Section III. The required frequency behaviors of the relative permittivity and permeability are compared with those attainable using existing materials.

Although the results provide no basis for optimism at the moment, some of the active network synthesis approaches for achieving the desired loading appear more promising. In Section IV various types of circuit are examined, with emphasis on the Negative Impedance Converter (NIC). An active load using a particular NIC circuit was constructed for use in the 5-10 MHz range and measured values of its performance have shown it capable of producing the loading required for at least a 13 dB cross section reduction over a 2:1 bandwidth. The advances in high performance transistors and in circuit techniques necessary to duplicate this achievement at a ten-fold larger frequency are discussed in Section VI.

II

BACKGROUND

The idea of using loading to reduce the reradiated fields dates back to the 1920's (Meissner, 1929), when it was common practice to use lumped inductors and capacitors to detune the supporting structures for broadcast transmitting antennas whenever their lengths were near resonance and interfered with the antenna radiation patterns. The first reported application of the loading technique for scattering reduction at microwave frequencies was by Iams (1950), who used a coaxial loading to decrease the scattering from metallic posts in a parallel-plate pillbox structure. King (1956) investigated the change in current distribution on a thin cylindrical rod when a central load is introduced, and later Hu (1958) and Ås and Schmitt (1958) showed that a high reactive impedance can appreciably affect the scattering behavior of such a rod.

Nevertheless, the potential of this technique as a means of cross section reduction in the resonance region was not appreciated until the early 1960's. Following a study at AFCRL, Sletten (1962) reported that for cylinders approximately $\lambda/2$ in length, and $\lambda/4$ and $\lambda/8$ in diameter, significant reductions in their broadside cross sections could be obtained by reactive loading at their centers, and shortly after, work was commenced at the Radiation Laboratory aimed at exploring the use of reactive (impedance) loading as a means of reducing the cross sections of thin and thick cylinders, spheres and spheroids.

In view of Sletten's work, the loading of a circular cylinder was studied first (Chen and Liepa, 1964). A thin circular cylinder of length ℓ, $0 < \ell < 2\lambda$, was chosen since adequate mathematical tools were already available (King, 1956) for an analysis of the scattering. An approximate solution of the integral equation for the current on the cylinder was obtained as a function of the central load, Z_L, and from this an expression for the far field was derived and computed. It was found that the back scattering cross section at broadside could be reduced to zero by appropriate choice of load, and that a non-zero resistive component, R_L, was

in general necessary for this purpose. It was further shown that for a cylinder of length $\ell < \lambda$ this optimum loading was passive ($R_L \geq 0$), whereas for a cylinder of length $\lambda < \ell < 2\lambda$ and active ($R_L < 0$) load was usually required. The corresponding reactive component X_L, in general, had a negative slope ($\partial X_L / \partial \omega < 0$). For cylinder lengths near resonance ($\ell \sim \lambda/2$) or shorter, a loading which decreases the back scattering at broadside also decreases the magnitude of the current induced in the cylinder by as much as 70 per cent, and, in consequence, this same loading reduces the bistatic scattering at all aspects other than end-on, as well as back scattering for oblique incidence. For a cylinder beyond resonance, however, the loading to reduce the back scattering cross section at broadside is not so effective for bistatic angles or for oblique incidence. The reason for this becomes clear when the dipole currents are examined for the case of oblique incidence. By dividing the current into components which are symmetric or anti-symmetric with respect to the center of the cylinder, it is obvious that a center load affects only the symmetric component and leaves the anti-symmetric one unaltered, suggesting that double loading would be desirable for this application. A theoretical investigation of a thin cylinder with two equal loads symmetrically placed was carried out by Chen (1965), who showed that loading positions could be found at which the impedances necessary to suppress the contributions to the back scattered field provided by both the symmetric and anti-symmetric modes were approximately the same. Under the stipulation of passive loading ($R_L \geq 0$), he found that the back scattering cross section could be significantly reduced at almost all angles of incidence for cylinders up to 1.5λ long. This suggests that if impedance loading is used to reduce the return from large bodies at all aspects, the loads should be placed not more than 0.75λ apart.

The impedance loading of a sphere was investigated next. The main reasons for choosing such a shape were the desire for a body having a carrying capacity, and one for which analyses could be carried out which are effectively exact regardless of frequency. Some of the uncertainties present in the analysis of even a thin cylinder of length greater than 2λ could now be avoided.

The particular case studied was that of a metallic sphere loaded with a slot in a plane perpendicular to the direction of incidence (Liepa and Senior, 1964, 1966). The slot was assumed to be of small but finite width with a constant electric field across it; under this assumption the analysis for the external fields was exact. Expressions for the scattered far field components as well as the total surface field components were derived, and these were used to investigate the modifications to the scattering cross section produced by various slot admittances. The numerical work was limited to the range $0 < ka \leq 10$, where k is the propagation constant of free space and a is the radius of the sphere.

It was found that the loading admittance necessary for any given modification is in general complex, with positive or negative real part corresponding to energy absorbing or radiating loads respectively. The loading required to reduce the back scattering cross section to zero was examined in some detail. It was shown that for any given slot position, the ranges of ka in which the real part of the loading admittance is negative or positive alternate with one another, with the locations of these bands being functions of the slot position. For example, with the slot at the shadow boundary ($\theta_0 = 90^\circ$), there are three negative bands in the range $0 < ka \leq 10$, but as the slot is moved towards the front of the sphere, these bands appear to slide in the direction of increasing ka.

At selected frequencies for which the demanded loading is reactive, the theoretical predictions were confirmed by measurements made using a sphere with a circumferential slot backed by a radial cavity whose depth could be varied by inserting discs of the appropriate diameter. Back scatter reductions in excess of 20 dB were observed, and measurements of both the surface and back scattered far fields as functions of angle for various reactive loads were performed to verify the theory.

Unfortunately, the variation of susceptance with frequency for the radial cavity (or any other sless network) is the direct opposite of that required to

reduce (or enhance) the back scattering cross section. As a result, the loading can be satisfied only where the two admittance curves intersect, and narrow bandwidths are therefore to be expected. To determine the actual bandwidths encountered with susceptive loading, the case when the sphere is loaded at the shadow boundary ($\theta_0 = 90^\circ$) for zero back scattering was examined at ka = 4.28. The required optimum loading and that supplied by a radial cavity (such as used in the experimental model) are shown in Fig. 2-1a. The depth of the cavity was chosen to produce this optimum loading at ka = 4.28. It is evident that the corresponding curves, especially for the real part, have completely different behaviors, and a minute deviation in frequency from the critical value therefore results in a large difference between the desired and the supplied loadings. The cross section corresponding to the cavity loading is shown in Fig. 2-1b. As expected, complete suppression is achieved at ka = 4.28, but the reduction is highly frequency sensitive. For example, for a 10dB reduction in the cross section, the bandwidth is 6.5 per cent and decreases to only 2 per cent when a 20 dB reduction in the cross section is desired.

It is obvious that the chances of achieving broadband loading are greatest in the frequency range where the variations of the required admittance are smallest. Fortunately, such a frequency range corresponds to the so-called resonant region where the back scattering cross section exhibits pronounced oscillations as a function of frequency. For example, with a slot of angular width 0.0332 radians and located at $\theta_0 = 60^\circ$, i.e. 30° forward of the shadow boundary, the real and imaginary parts of the normalized loading admittance that must be provided at the slot to produce zero back scattering are shown as functions of ka in Fig. 2-2. It is at once apparent that the variation of the susceptance as a function of frequency (or ka) has primarily a negative slope and is, in fact, almost the reverse of that provided by a typical cavity. It is therefore not surprising that when one attempts to generate the required loading using elementary devices, radar cross section reductions can be achieved over a bandwidth of a few percent at most.

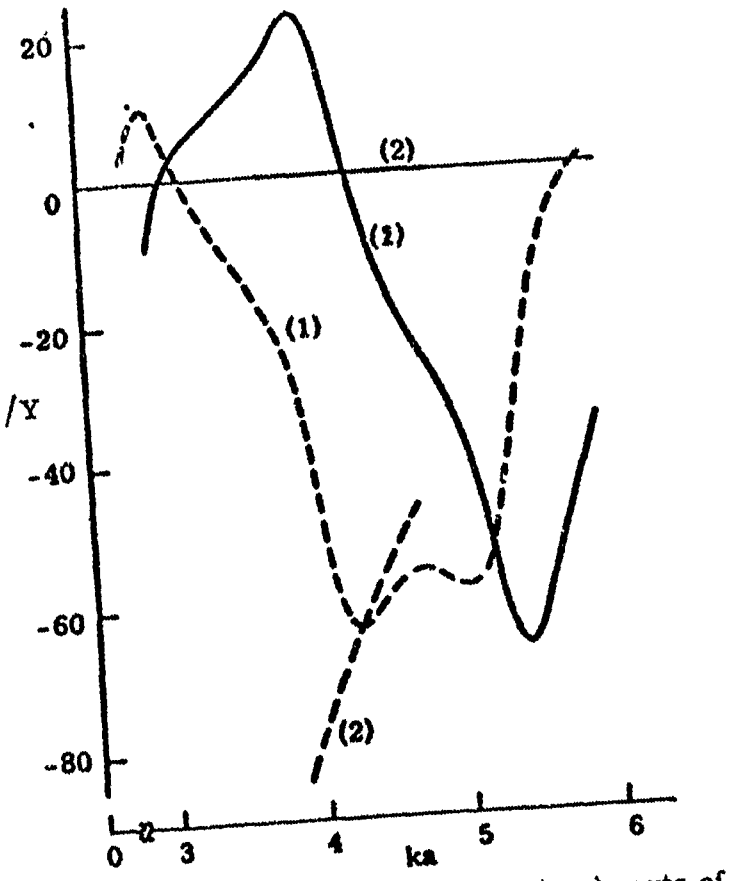

FIG. 2-1a: Real (—) and imaginary (---) parts of (1) normalized loading admittance for zero back-scattering with $\theta_o = 90^o$ and (2) loading supplied with lossless radial cavity.

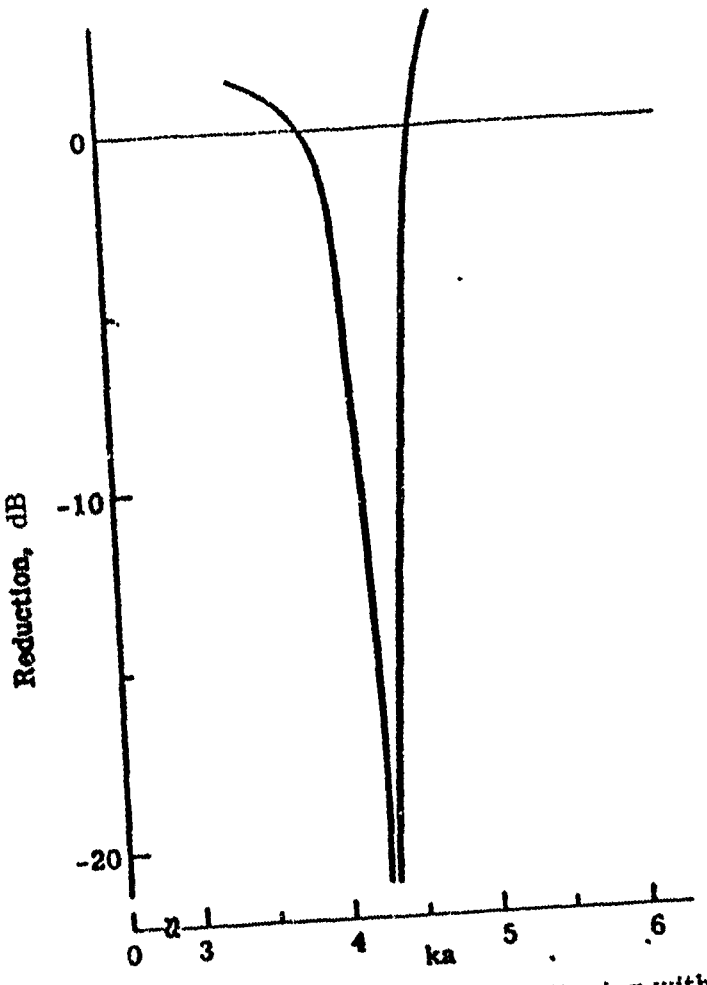

FIG. 2-1b: Reduction in back scattering with susceptive loading at $\theta_o = 90^o$.

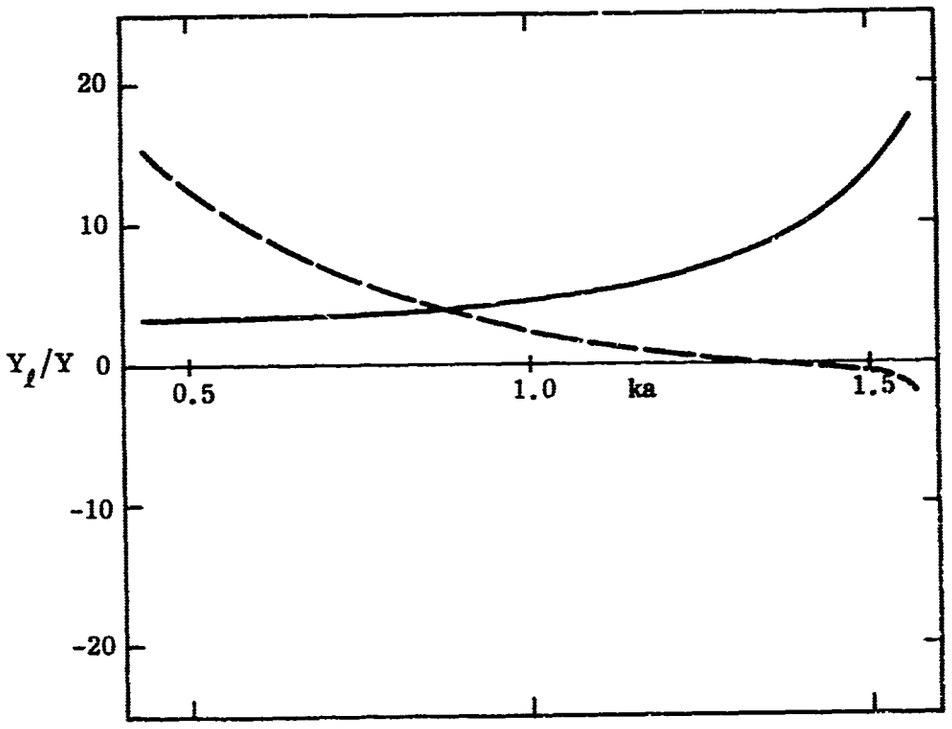

FIG. 2-2: Real (——) and imaginary (---) parts of the optimum loading admittance for zero back scattering with $\theta_o = 60^o$.

The orientation of the sphere loading considered by Liepa and Senior (1964, 1966) is analytically convenient since only the tesseral harmonics of the first order appear in the expressions for the surface and far fields. Practically, however, the choice is not so desirable. The fact that the voltage appearing across the slot has an asymmetric ($\cos\phi$) distribution means that the loading must be distributed around the slot and cannot be lumped as a single load at the center of the cavity where the voltage is zero. In order to reduce the complexity of the practical loading problem, the treatment of Liepa and Senior was now extended to the case of an azimuthally-loaded sphere at arbitrary incidence (Chang and Senior, 1967). The analysis paralleled in large measure that previously given, the only major difference being the occurrence of doubly-infinite sets of modes. Analytical expressions for the surface and far field components were presented, as well as for the loading necessary to produce selected forms of cross section control. Once again emphasis was placed on the reduction of the back scattering cross section, and in general there is now the choice of loading each mode so as to suppress its individual contribution, or of loading one mode (taking into account the effect, if any, of that load on all other modes) so as to suppress the net contribution in the far field. Practically, however, the former type of load would be almost impossible to realize, and since a load placed at the center of a radial cavity affects only the zero order mode, it is most convenient to load in this manner whenever the zero order mode is present, i.e. for all angles of incidence other than normal to the slot.

In both the numerical and experimental work, attention was concentrated on the case of a circumferentially-loaded sphere with the slot in the plane of incidence and normal to the incident electric vector. In the lower resonance region at least, the zero order mode is then the dominant contributor to the far field back scattering of the unloaded sphere, and adequate cross section control can be achieved using a single lumped load at the center of a radial cavity. The real and imaginary parts of the impedance at the center necessary to give zero back scatter were computed as functions of ka, and in Fig. 2-3 the curves are reproduced for the case of a

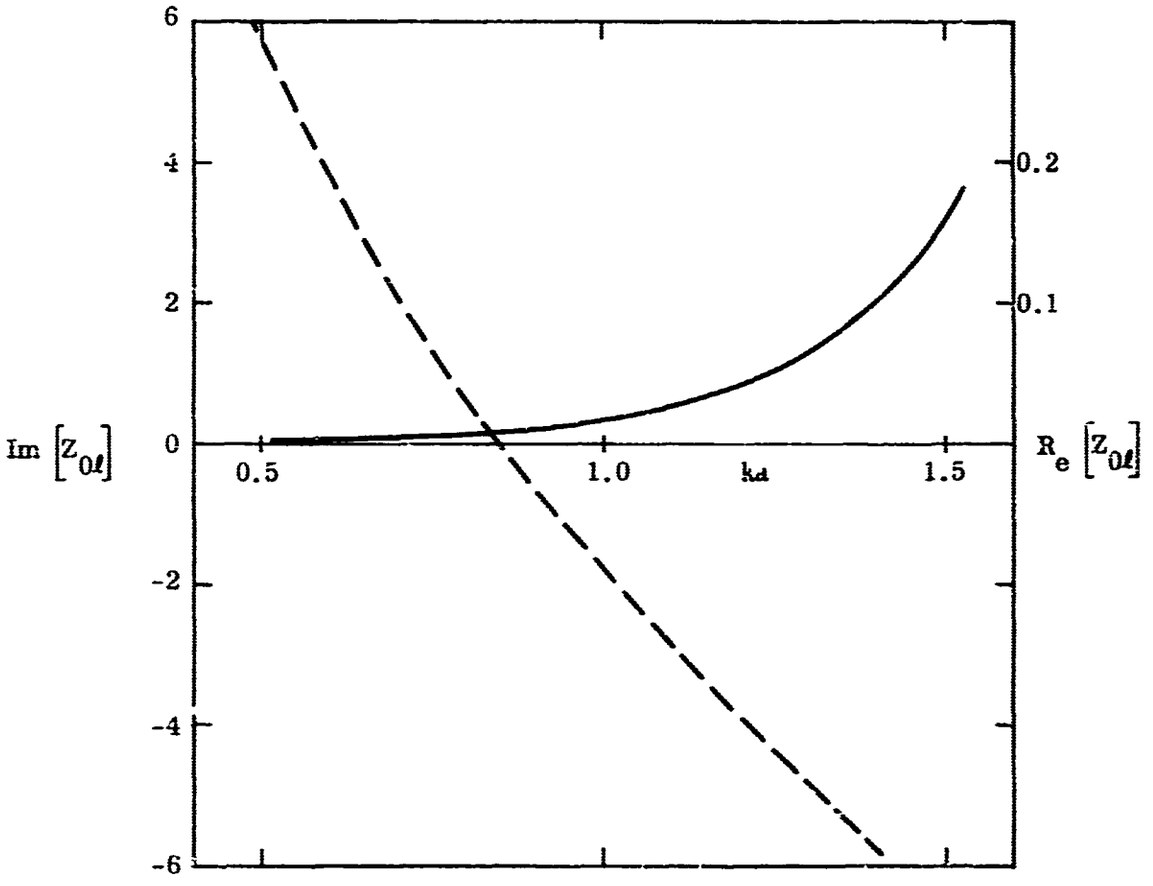

FIG. 2-3: Real (——) and imaginary (----) parts of the optimum loading impedance at the center of a sphere for zero back scattering.

slot of width 0.0399 radian. Again the reactive part of the demanded load exhibits the negative slope common to all the cases considered.

Closely related to the problem of narrow bandwidth is the extremely tight tolerance on the loading which is presented if the desired reductions in the radar cross section are to be obtained. McMahon (1969) computed the back scattering from a sphere with various loading impedances, and by plotting cross section contours for each frequency (or ka) on the impedance plane, he found that to produce a reduction in the back scattering cross section of at least 13 dB, the real and imaginary parts of the load must be within $\pm 0.1\,\Omega$ of their optimum values (Fig. 2-3). It follows that whatever means are used to produce the loading, very tight control must be exercised over the circuit components and/or loading materials.

Another approach to the loading problem that should be mentioned here is the compensation method in which the scattering of a body is modified by attaching external scatterers which are in turn loaded by impedances. The advantage of such a method is that the loading of the body is accomplished externally and thus the parent body does not have to be modified by cutting slots in the surface as in the cases discussed above. Chen (1965) used the compensation method to minimize the back scattering of a conducting cylinder by attaching a thin loaded wire near to the surface. Later, Chen and Vincent (1968) used the same technique to modify the radar cross section of a metallic sphere by attaching two thin, loaded monopoles on the opposite side of the sphere. In both cases it was found that the impedance required to annul the back scattering cross section is qualitatively the same as that for a slot cut into the surface of the body; in particular, the slope of its reactive part is still negative.

III

USE OF FREQUENCY-DEPENDENT MATERIALS

A possible (though not necessarily realizable) method to achieve the desired loading over a significant frequency band is to consider a cavity filled with a homogeneous isotropic material of complex permeability and permittivity, and then allow these constants to vary as a function of frequency in order to obtain the desired impedance. Two cases have been studied: (a) the loading of a radial cavity and (b) the loading of a TEM transmission line. The results are presented in this Section.

3.1 Loading of a Radial Cavity

The original boundary value problem for this case was studied by Liepa and Senior (1966) and ended by specifying the real and imaginary parts of the loading admittance required to annul the back scattering cross section of the sphere. Consider the case of a slot at $\theta_0 = 60^\circ$ (i.e. 30° forward of the shadow boundary) of angular width 0.0392 radian. The real and imaginary parts of the normalized loading admittance Y_l/Y that must be provided for zero back scattering are shown as functions of ka in Fig. 2-2. A method of generating the required admittance is to back the slot with a radial cavity. Liepa and Senior did this in their experimental study, but due to the incompatability of the admittance demanded and that supplied by the radial cavity, the demanded loading could be supplied only at spot frequencies. It is this incompatability that results in the narrow band performance of the loaded sphere (cf. Fig. 2-1, for example) and of the impedance loading technique in general.

If the radial cavity is loaded with a material whose electric properties vary with frequency, what would be the demands on this frequency variation? To answer this question, a study was performed (Senior and Knott, 1967a, b) of a radial cavity backing the slot and filled with a homogeneous isotropic material of complex (relative) permittivity ϵ_r and permeability μ_r. The input admittance, relative to free space, of such a cavity is given by

$$Y_\ell/Y = -2\pi i \frac{k_r}{\mu_r} \frac{a}{d} \frac{J_1'(k_r ka)N_1(k_r kb) - N_1'(k_r ka)J_1(k_r kb)}{J_1(k_r ka)N_1(k_r kb) - N_1(k_r ka)J_1(k_r kb)} \qquad (3.1)$$

where d is the width of the cavity. b is the radius of the inner short, and

$$k_r = \sqrt{\epsilon_r \mu_r} \quad . \qquad (3.2)$$

The values of the parameters a and d are fixed by the model and henceforth we shall take

$$a/d = 25.064 \quad . \qquad (3.3)$$

corresponding to a slot of angular width 0.0392 radian. The parameter b can be varied, but once a value has been chosen, it is assumed that it cannot be changed to produce any impedance variation.

Using a combined analytical-graphical approach, Senior and Knott computed values for μ_r and ϵ_r which, when inserted in Eq. (3.1), would generate the optimum loading admittance value given in Fig. 2-2. The computation was a rather involved and lengthy one and we shall therefore present only the results. Fig. 3-1 shows the real and imaginary parts of the relative permittivity ϵ_r and relative permeability μ_r necessary to achieve the desired loading. The condition $\mu_r = \epsilon_r$ is not essential, but does limit the data to one pair of curves; it also maximizes the minimum loss tangent over the range, and minimizes the total variations of the real parts of μ_r and ϵ_r. In general it is seen that the real part of the required $\mu_r = \epsilon_r$ is a decreasing function of frequency varying from about 4.6 to 1.4 over the frequency range considered, and the corresponding imaginary part has an inverted bell-shape behavior with an average value of about 0.06.

In searching for such a material, various books, reports, etc., have been consulted and the problem has been discussed with a ferrite manufacturing group, but unfortunately no material has been found which exhibits the frequency behavior appropriate to the optimum loading. Some ferrite materials do exhibit a frequency

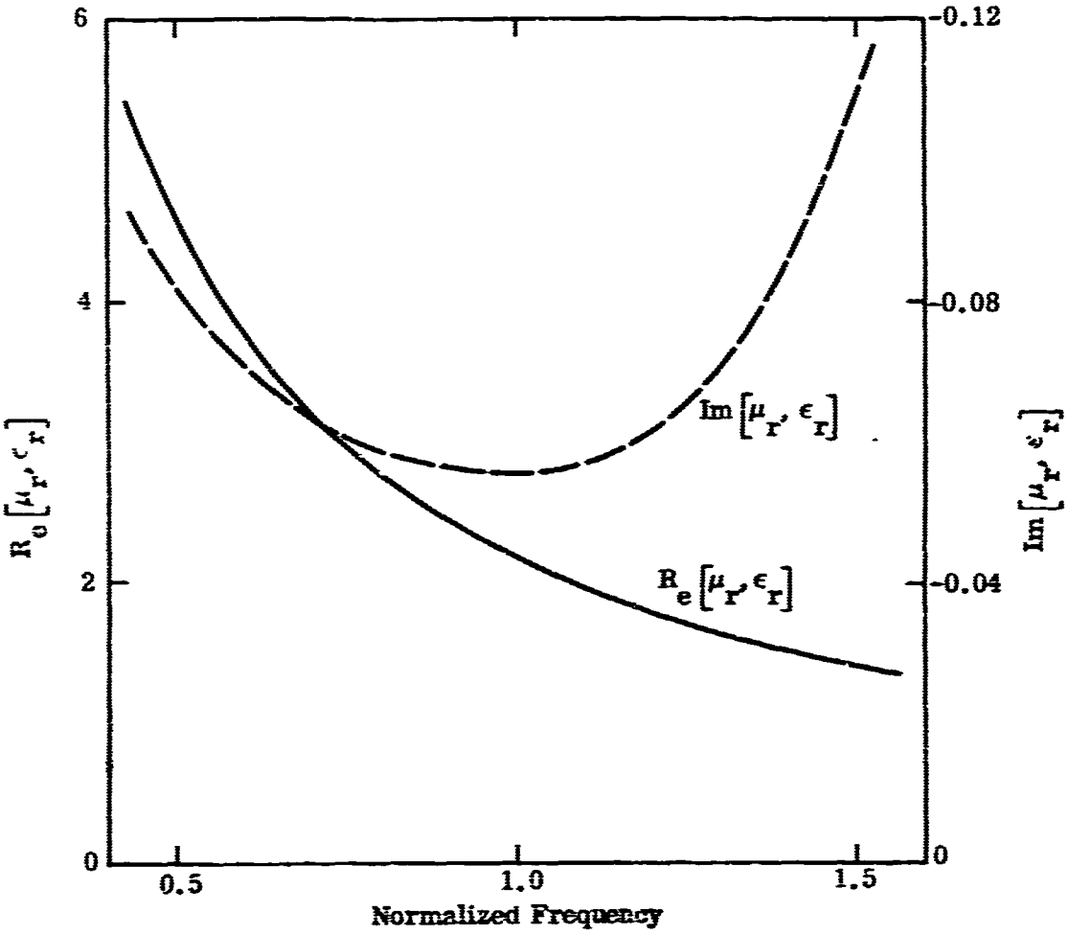

FIG.3.1:Real and imaginary parts of μ_r, ϵ_r necessary to achieve the required impedance in a radial cavity when $\mu_r = \epsilon_r$.

variation whose real parts resemble that demanded, but they also possess imaginary parts of the same order of magnitude as the real parts. As such, the imaginary parts are about two orders of magnitude larger than those required for optimum loading (see, for example, Smit and Wijn, 1959).

What cross section reduction can be expected if we place in the cavity a material whose real part matches that demanded, but whose imaginary part is greater by two orders of magnitude? This particular aspect of the problem has not been studied directly, but judging from the negative results of a related experimental study (Senior and Knott, 1967a) in which a cylindrical structure was loaded with lossy dielectric material to reduce its cross section over an extended frequency range, as well as the study of loading impedance tolerances for a sphere (McMahon, 1969), one could expect at most a few dB reduction in cross section. In fact, depending on the frequency, an enhancement in cross section could occur.

3.2 Loading of a TEM Transmission Line

In this Section we examine how the electrical properties of materials placed in a transmission line (coaxial cavity) of fixed length must vary with frequency to produce at the line input the desired impedance over a significant frequency range. Specifically, the impedance desired is that required for zero back scattering in the case of a sphere loaded at the equator with a circumferential slot perpendicular to the incident electric field vector. The slot is backed by a radial cavity which, in turn, is terminated at the center by an impedance Z_{0f}. This is then the impedance that must be realized if a cross section reduction over a given frequency range is to be achieved.

To simplify the formulation, as well as the computation, assume that the impedance Z_{0f} is generated by a coaxial cavity uniformly filled with a homogeneous isotropic material whose electric properties are to be determined to produce Z_{0f}. The expression for the input impedance of a segment of a transmission line is well known, but is usually given for the case when the transmission line is lossless

(cf. Ramo and Whinnery, 1958). However, the same formula can also be used when the line is filled with a lossy material by allowing the permittivity and permeability to take on complex values. In this case, the input impedance is given by

$$Z_{in} = Z_r Z_0 \frac{Z_\ell \cos(k_r k\ell) + jZ_r Z_0 \sin(k_r k\ell)}{Z_r Z_0 \cos(k_r k\ell) + jZ_\ell \sin(k_r k\ell)} \quad , \tag{3.4}$$

where

$Z_r = \sqrt{\mu_r/\epsilon_r}$: relative characteristic impedance of the line,

Z_0 = characteristic impedance of the line when unloaded,

Z_ℓ = terminating impedance for the line,

$k_r = \sqrt{\mu_r \epsilon_r}$: relative propagation constant,

k = free space propagation constant,

and ℓ = length of the line.

Both μ_r and ϵ_r are complex, and because they are contained in the sine and cosine functions as well as the expression for Z_r, it would be very difficult (even in special cases) to solve for μ_r and ϵ_r explicitly. To determine the optimum μ_r and ϵ_r corresponding to the required input impedance, an error function ϵ was defined as

$$\epsilon = \left| Z_{0\ell} - Z_{in} \right| \quad , \tag{3.5}$$

where Z_{in} is given by Eq. (3.4), and $Z_{0\ell}$ is the impedance that must be generated by the loaded line at each of several specified frequencies. The computation of the optimum impedance $Z_{0\ell}$ for zero back scattering was carried out by Chang and Senior (1967) and the results are presented in Fig. 2-3. They are also repeated in Table 3.1 where the values are given to 4 significant figures. Note that even though the loading in this case is at the center, and the problem is different from that considered in Section 3.1 in that the slot is normal to the incident electric field

vector instead of normal to the direction of incidence, the general character of the optimum impedance is still the same—the imaginary or reactive part has a negative slope and the real part is small and positive.

TABLE 3.1

Optimum Impedance for Zero Back Scattering

ka	$\mathrm{Re}\left[Z_{0\ell}\right]$	$\mathrm{Im}\left[Z_{0\ell}\right]$
0.5	$.7860 \times 10^{-3}$	5.798
0.6	$.1705 \times 10^{-2}$	3.709
0.7	$.3322 \times 10^{-2}$	2.034
0.8	$.5982 \times 10^{-2}$	0.615
0.9	.01016	-0.638
1.0	.01653	-1.780
1.1	.02616	-2.844
1.2	.04086	-3.857
1.3	.06392	-4.837
1.4	.1015	-5.805
1.5	.1610	-6.792

To determine the required variations of μ_r and ϵ_r as functions of frequency, Eq. (3.5) was solved numerically on a computer using an optimization process to minimize ϵ. For computational purposes the condition on ϵ was preset to $\epsilon \leq 0.1$ which limited $Z_{0\ell}$ to a maximum departure of $\pm 0.1\,\Omega$ from optimum. The values for the other parameters were $Z_0 = 50\,\Omega$, $Z_\ell = 0\,\Omega$, and a cavity length ℓ such that at ka = 1 (which corresponds to unity on a normalized frequency scale) the electrical line length is about half a wavelength. This restricted the amplitudes of μ_r and ϵ_r to a range from 1 to 10 over the frequency band considered.

Since microwave cavities may support multiple modes, some convergence difficulties were experienced in obtaining solutions corresponding to the lowest order mode. In addition, when μ_r and ϵ_r are allowed to vary independently, a unique solution for a given frequency and cavity depth does not exist. For this reason, an additional restriction was placed on μ_r and ϵ_r, namely, $\mu_r = \epsilon_r$, $\mu_r = 2\epsilon_r$, or $\mu_r = \frac{1}{2}\epsilon_r$, and in these special cases it was found possible to compute the variations in μ_r and ϵ_r required to provide the desired frequency response for the cavity.

In Fig. 3-2, the computed values are shown when $\mu_r = \epsilon_r$. Over the frequency range considered (0.5 to 1.5), the real part of $\mu_r = \epsilon_r$ changes from about 4.2 to 1.25 and the imaginary part (i.e. the loss) of $\mu_r = \epsilon_r$ changes from about 0.1×10^{-3} to 1.3×10^{-3}. In Figs. 3-3 and 3-4, the results are presented for $\mu_r = 2\epsilon_r$ and $\mu_r = \frac{1}{2}\epsilon_r$, respectively. At first glance it appears that the curves in the two figures are the same except for interchanged μ_r and ϵ_r. An examination of the actual numbers, however, reveals that the curves are slightly different and this can be seen by observing that in Eq. (3.4) the impedance of the cavity depends on both factors $\sqrt{\mu_r}/\sqrt{\epsilon_r}$ and $\sqrt{\mu_r \epsilon_r}$, where the former is dependent on the ratio of μ_r to ϵ_r and the latter (being a product of μ_r and ϵ_r) is not.

As was the case for the problem treated in Section 3.1, no real-life materials that satisfy the demanded frequency variation appear to exist. In fact, the demands on the material appear even worse here. Although materials are available whose real parts resemble those required, they also possess imaginary parts of order unity or greater. In contrast, for the computations carried out, the imaginary parts of μ_r or ϵ_r must be of order 10^{-1} in the case of a radial cavity (Section 3.1) and of order 10^{-3} when the load is transferred as a lumped element to the center and realized by a TEM transmission line (Section 3.2).

In the hope of requiring properties of dielectric/magnetic materials that are more realistic than those obtained above, cases were investigated where the transmission line is terminated in loads other than $Z_\ell = 0$. To limit the number of

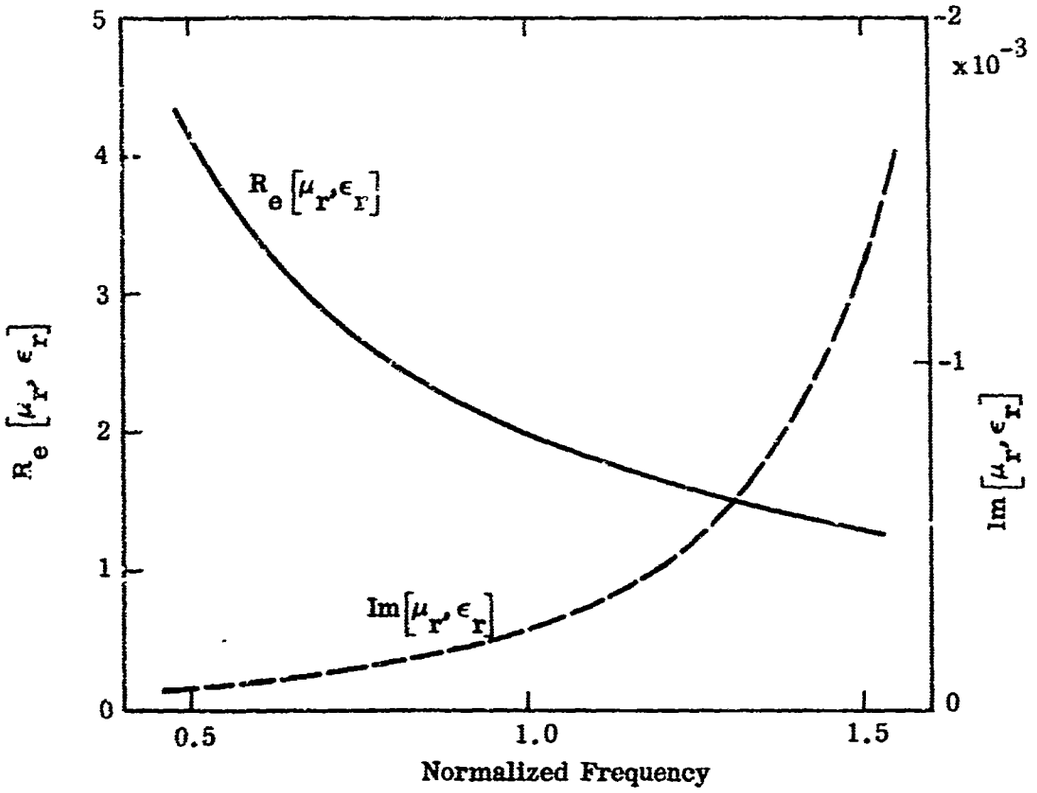

FIG. 3.2: Real and imaginary parts of μ_r, ϵ_r necessary to achieve the required impedance in a shorted transmission line when $\mu_r = \epsilon_r$.

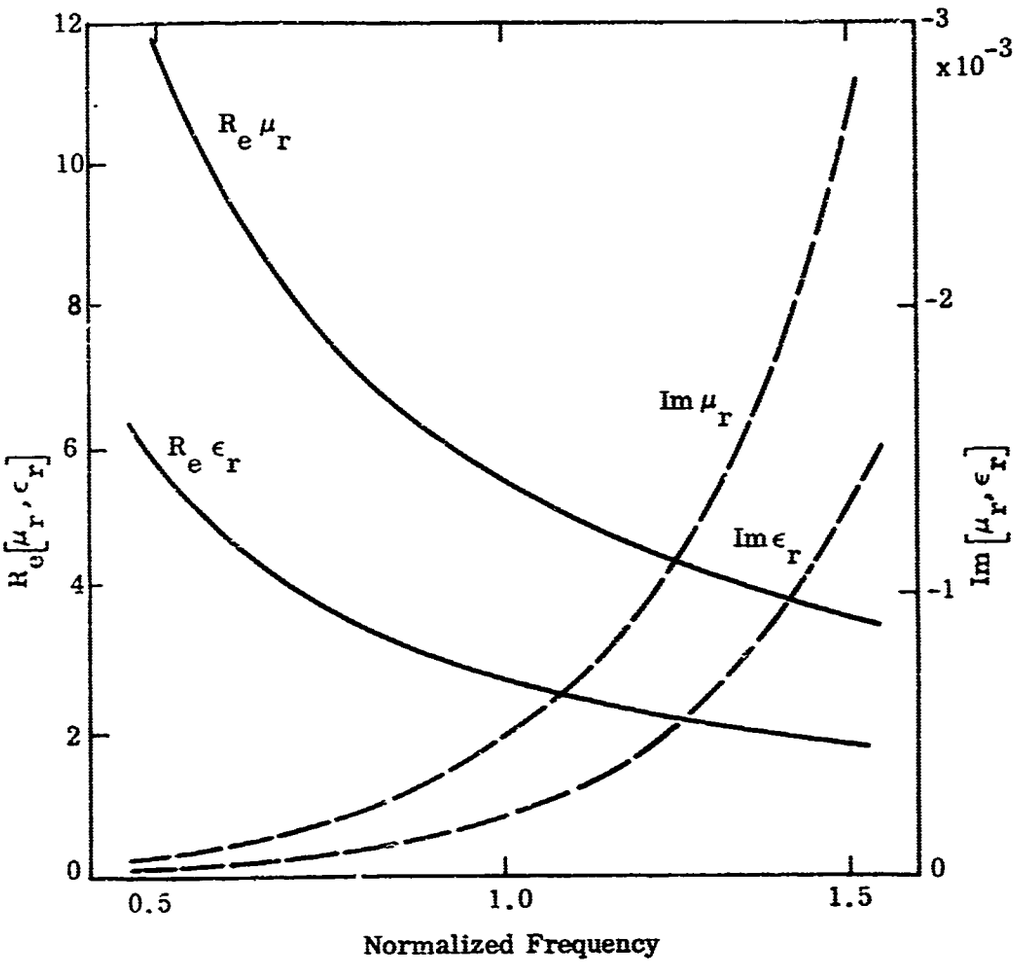

FIG. 3.3 Real and imaginary parts of μ_r, ϵ_r necessary to achieve the required impedance in a shorted transmission line when $\mu_r = 2\epsilon_r$.

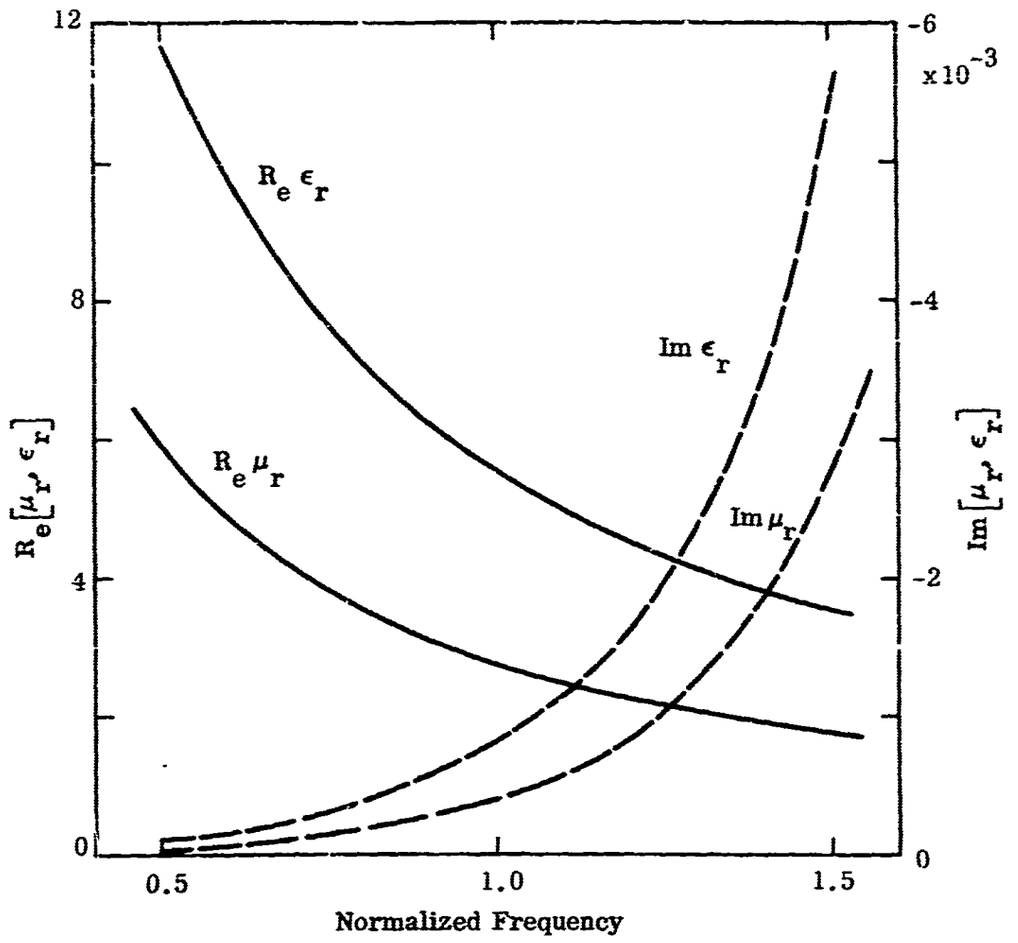

FIG. 3. 4 Real and imaginary parts of μ_r, ϵ_r necessary to achieve the impedance in a shorted transmission line when $\mu_r = \frac{1}{2}\epsilon_r$.

computations, the condition $\mu_r = \epsilon_r$ was chosen, and computations were performed similar to those described above, but for terminations which were

a) resistive,

b) open circuit,

c) inductive,

and d) capacitive.

In all of the cases considered, the curves for μ_r and ϵ_r resembled those shown in Fig. 3-2: the real part decreased with frequency while the (small) imaginary part (except when the load was resistive) increased. For a resistive load, the required imaginary part was positive, implying an "active" material which is obviously non-existent. Since the curves for the required $\mu_r = \epsilon_r$ are so similar to those of Fig. 3-2, the appropriate curves will not be presented, but only the ratios of max to min values of $\mu_r = \epsilon_r$ demanded over the 0.5 to 1.5 frequency range. Such ratios may eventually be of interest, since for all known low-loss materials, the permeability and permittivity are almost constant with frequency. The short

Z_ℓ	Max to Min Ratios of $\mu_r = \epsilon_r$
Short	3.26
Open	3.53
Capacitive (C = 0.01 Farads)	3.27
Inductive (L = $24/\pi$ Henries)	3.28

circuit line appears to be the best of the cases considered, although the ratios for inductive or capacitive loading are not much greater. Values of L and C other than those used above were also examined, but the results were the same—the short circuited load still gave the smallest max to min ratio.

The unrealistic requirement on the variation of μ_r and ϵ_r as a function of frequency to produce zero back scattering is hardly surprising. As shown by McMahon et al (1968), the required impedance cannot be obtained using passive lumped elements, and this would lead us to expect that passive distributed networks

would also be ineffective. Furthermore, if $\mathrm{Re}\left[Z_{0\ell}\right] = 0$, Foster's Reactance Theorem, stating that

$$\frac{\partial \mathrm{Im}\left[Z_{0\ell}\right]}{\partial \omega} \geq 0 \ , \tag{3.6}$$

where ω is the angular frequency, applies also for distributed loads (Ramo and Whinnery, 1958), and since the curve for the demanded impedance $Z_{0\ell}$ in Fig. 2-3 shows that

$$\frac{\partial \mathrm{Im}\left[Z_{0\ell}\right]}{\partial \omega} < 0 \ , \tag{3.7}$$

it would appear that such a load cannot be realized using passive devices. However, the optimal $Z_{0\ell}$ does have a non-zero real part albeit small, and under these conditions Foster's Reactance Theorem does not apply. It was for this reason that we proceeded to determine the electric characteristics of materials required for loading a coaxial cavity in the hope that the appropriate materials might exist or eventually be realized.

IV

CENTER LOADING

4.1 Introduction

The impedance required at the center of a conducting body to achieve cross section modification naturally differs from that required at the surface, since a center load must be coupled to the surface through a radial transmission line. However, the difference is quantitative rather than qualitative; the center load still has the general behavior of a negative reactance. For the particular case of a sphere, studied by Chang and Senior (1967), the required load can be well approximated by

$$Z(s) = -K \frac{s^2 + \omega_0^2}{s} \tag{4.1}$$

which for convenience may be normalized to

$$Z(s) = - \frac{s^2 + 1}{s} \quad . \tag{4.2}$$

The load may also be viewed as a reflection coefficient

$$\rho = \frac{Z - Z_0}{Z + Z_0} = \frac{s^2 + s + 1}{s^2 - s + 1} \tag{4.3}$$

where Z_0 has been normalized to unity. For $s = j\omega$, we have

$$|\rho| \equiv 1 \tag{4.4}$$

and

$$\angle\rho = 2 \tan^{-1} \frac{\omega}{1 - \omega^2} \quad . \tag{4.5}$$

Although there is a one-to-one correspondence between load impedance and reflection coefficient, the reflection coefficient viewpoint is perhaps more appropriate to an understanding of the mechanisms involved, since cross section reduction is achieved basically by changing the phase of the current over a portion of the scatterer to obtain cancellation of the scattered field in a prescribed direction.

4.2 Reflection Coefficient Realization

In view of Eqs. (4.4) and (4.5), the loading may be viewed as a mechanism for reflecting the incoming wave with its magnitude unchanged but with the phase changed in a prescribed manner. One way in which this might be done is shown in Fig. 4-1, where an ideal circulator is combined with an all-pass, phase-shift

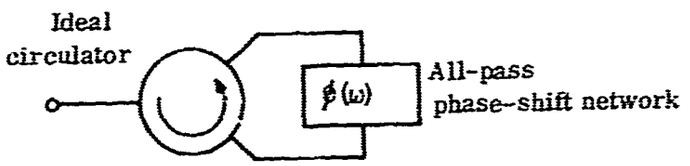

FIG. 4-1: Reflection Coefficient Realization.

network. Quite aside from the difficulty of realizing a broad-band, high-frequency circulator, this scheme is doomed to failure by a fundamental limitation of all-pass networks. The transmission function of any all-pass network, passive or active, is of the general form

$$H(s) = K \frac{(s-s_1)(s-s_2)\ldots}{(s+s_i)(s+s_2)\ldots} \qquad (4.6)$$

where the s_i have positive real parts; in other words, there are poles in the left half plane, with zeros at the mirror-image right half-plane points. The angle of any rational function at any point s_0 is the sum of the angles (measured in the usual counterclockwise direction) from all the zeros to s_0, minus the sum of the angles from the poles. When a function having the form of Eq. (4.6) is evaluated on the $j\omega$ axis, the zeros are all to the right and the poles all to the left. Therefore, the zero angles are all decreasing, and the pole angles increasing, as frequency increases. A stable all-pass function thus has a phase shift which decreases with frequency; however, the phase-shift function (Eq. (4.5)) is an increasing function of frequency and therefore cannot be realized by an all-pass network.

Minimum phase networks, having both poles and zeros in the left half s-plane, can realize phase shifts which increase with frequency. In this case, however, the magnitude function cannot be maintained at a constant value. It must be concluded therefore, that the reflection coefficient to provide the desired reflection cannot be realized by a passive network. An active realization based on the reflection coefficient approach does not appear to offer any advantage over a realization based on the impedance approach, which is discussed below.

4.3 Impedance Realization

There are a number of active elements with the potential for realizing the desired impedance given by Eq. (4.1). Some which have been considered and rejected are discussed below.

Pumped varactor diodes are known to exhibit input impedances not realizable by passive networks, which suggests their possible application to the problem at hand. Unfortunately, the variation of impedance with frequency is difficult to predict and extremely difficult to control, since it depends on a relatively large number of parameters. While there may be cases for which varactor diodes provide a suitable load, it is unlikely that the probability of success justifies the effort which would be involved.

Suitably-biased tunnel diodes yield a negative-resistance characteristic which has been exploited in a number of active synthesis schemes. Since the negative resistance is always shunted by a parasitic capacitance, tunnel diode realizations are more limited in generality than some other active realizations. There is also a severe stability problem due to the presence of lead inductance, which tends to make the device self-resonant at some fairly high frequency. For these reasons, the tunnel diode would appear to offer no advantage, and some disadvantages, when compared with other possible methods.

Two other possibilities which are worth mentioning are nonlinear and adaptive realizations. Nonlinearity can be discarded immediately, since the strength of the incident wave is not constant and a nonlinear load would, by definition, have a response dependent on signal amplitude.

An adaptive loading scheme, in which the frequency of the incoming signal is sensed and acts as the control signal for a discrete or continuous tuning system, has some obvious advantages and disadvantages. Since a relatively large number of load parameters can be made to vary more or less arbitrarily, almost any impedance variation can be achieved. On the other hand, such a scheme would probably involve time delays on the order of milliseconds, which could be unacceptable in some applications and would certainly be ineffective if the incoming signal were broadband or swept in frequency. In any event, adaptive schemes were felt to be outside the scope of our investigations and were not considered in any detail.

4.4 The Negative Impedance Converter

Of the active devices which are applicable to general synthesis techniques, the one most suitable for the present problem would appear to be the Negative Impedance Converter, or NIC.

The NIC is, of course, only one of many devices which have been used for active synthesis. Of the other possibilities, the gyrator may be ruled out immediately, since the class of driving-point impedance functions realizable with a gyrator is also realizable with passive elements only (the gyrator does, however, offer advantages in transfer function synthesis). Realizations using controlled sources, operational amplifiers, etc., handle the same class of functions as do NIC realizations and in fact frequently lead to networks embodying a NIC; there is thus no loss of generality if these realizations are not treated separately.

4.5 NIC Theory

The Negative Impedance Converter, or NIC, is a two-port with the property that the impedance seen at one port is the negative of the impedance terminating the other port. The NIC is most conveniently characterized by its h-parameters, which have the general form

$$\begin{bmatrix} V_1 \\ I_2 \end{bmatrix} = \begin{bmatrix} h_{11} & h_{12} \\ h_{21} & h_{22} \end{bmatrix} \begin{bmatrix} I_1 \\ V_2 \end{bmatrix} \tag{4.7}$$

With port 2 terminated by an admittance Y_2, the input impedance is given by

$$Z_1 = h_{11} - \frac{h_{12}h_{21}}{h_{22}+Y_2} \quad . \tag{4.8}$$

In order to operate as an NIC, the two-port must have the properties

$$h_{11} = h_{22} = 0 \tag{4.9}$$

$$h_{12}h_{21} = 1 \quad . \tag{4.10}$$

In practice, the latter condition is normally satisfied by

$$h_{12} = h_{21} = \pm 1 \tag{4.10}$$

with the positive sign yielding a current-inverting NIC (INIC) and the negative sign a voltage inverting NIC (VNIC). Many NIC circuits have been given in the literature; most of them are essentially realizations of one of the two circuits shown in Fig. 4-2, where equivalent circuits for the ideal INIC and VNIC are shown.

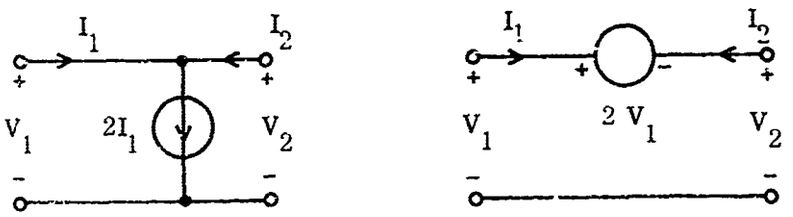

FIG. 4-2: Basic NIC Realizations.

Given an ideal NIC, the most obvious way of realizing the desired impedance is to terminate the NIC with a series-resonant circuit. Quite apart from the usual difficulties associated with inductors, such as losses and stray capacitance, this scheme is generally unsatisfactory if the NIC is not perfect. Except at very low frequencies, the conversion ratio of the NIC will normally be a complex function of frequency; that is

$$\frac{Z_{in}}{Z_{load}} \triangleq k = a(\omega) + jb(\omega) \tag{4.12}$$

where $a(\omega)$ is negative and $b(\omega)$ is small compared to $a(\omega)$. A purely reactive load then yields

$$Z_{in} = (a+jb)\, jY_L = -bY_L + jaY_L \tag{4.13}$$

which has an undesirable real component. If resistance is added to the load in an attempt to compensate, the result is

$$Z_{in} = (a+jb)(R_L + jY_L) = (aR_L - bY_L) + j(aY_L + bR_L)\ . \tag{4.14}$$

The condition for making Z_{in} purely reactive, namely

$$aR_L - bY_L = 0\ , \tag{4.15}$$

in general cannot be satisfied with $R_L > 0$ over a frequency band in which Y_L changes sign unless b changes sign simultaneously with Y_L. Since $b(\omega)$ cannot normally be controlled to such an extent, compensation cannot be achieved with this realization.

Fortunately, there exist realization techniques which not only avoid the use of inductors but which also offer better potential for compensation. By subtracting an appropriate positive resistance from the normalized $Z(s)$ we obtain

$$Z_1(z) = Z(s) - (a+\frac{1}{a}) = -\frac{s^2+1}{s} - (a+\frac{1}{a}) = \frac{s^2+(a+\frac{1}{a})s+1}{s} \tag{4.16}$$

which has simple, negative-real zeros. Then, by expanding $Y_1(s)$ as an RC admittance, one obtains

$$Y_1(s) = \frac{as}{(s+\frac{1}{a})(1-a^2)} - \frac{as}{(s+a)(1-a^2)} \tag{4.17}$$

where it has been assumed, without loss of generality, that $a < 1$. Since $Y_1(s)$ has been expressed as the difference of two RC admittances, it can be realized with an NIC. Adding on the constant originally subtracted leads to the final realization shown in Fig. 4-3.

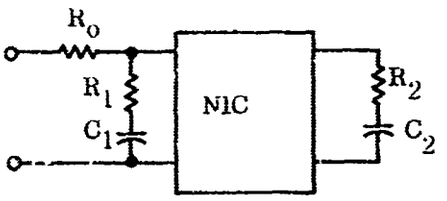

with $R_0 = \frac{1+a^2}{a}$ $\qquad R_1 = \frac{1-a^2}{a}$ $\qquad R_2 = \frac{1-a^2}{a}$

$C_1 = \frac{a^2}{1-a^2}$ $\qquad C_2 = \frac{1}{1-a^2}$

FIG. 4-3: RC - NIC Realization of Z(s).

The dual procedure to the above approach also leads to a realization. Subtracting a suitable positive constant from Y(s) yields

$$Y_1(s) = Y(s) - \frac{a}{1+a^2} = -\left(\frac{a}{1+a^2}\right)\frac{(s+a)(s+\frac{1}{a})}{s^2+1} \quad . \tag{4.18}$$

As before $Z_1(s)$ may be expanded as an RC impedance, yielding

$$Z_1(s) = -\frac{(1+a^2)^2}{a(1-a^2)}\left\{\frac{1-a^2}{1+a^2} + \frac{a}{s+a} - \frac{1/a}{s+\frac{1}{a}}\right\} \tag{4.19}$$

which is the difference of two RC impedances and can therefore be realized using an NIC. The resulting realization is given in Fig. 4-4.

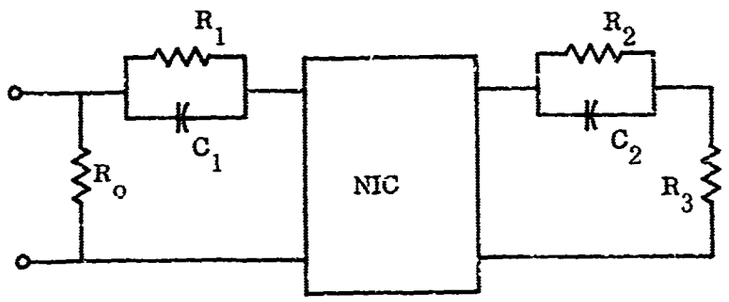

with

$$R_0 = \frac{1+a^2}{a} \qquad R_1 = \frac{(1+a^2)^2}{a(1-a^2)} \qquad R_2 = \frac{(1+a^2)^2}{a(1-a^2)} \qquad R_3 = \frac{1+a^2}{a}$$

$$C_1 = \frac{a^2(1-a^2)}{(1+a^2)^2} \qquad C_2 = \frac{1-a^2}{(1+a^2)^2}$$

FIG. 4-4: Alternate RC - NIC Realization.

In both of the realizations above, the parameter a may be chosen anywhere in the range $0 < a < 1$, the choice being determined by stability, element-value spread, etc. In practice, a value of $a = 0.5$ has proven to be a reasonable choice.

These realizations have an advantage over the LC realization in that the load impedance of the NIC, and therefore the input impedance as well, remains in one quadrant of the complex Z-plane. For example, in the first realization, as frequency varies, the load impedance moves along a vertical line in the fourth quadrant, as shown in Fig. 4-5a. With an ideal NIC, the input impedance would lie on a vertical line in the second quadrant, as shown by the solid line. If the NIC is non-ideal, the input impedance might have the form shown by the dotted line, which would result if the conversion ratio of the NIC had a phase angle which departed from 180° at the higher end of the frequency band. This effect could be compensated by changing the

load impedance, as shown in Fig. 4-5b. Since the modified load-impedance locus

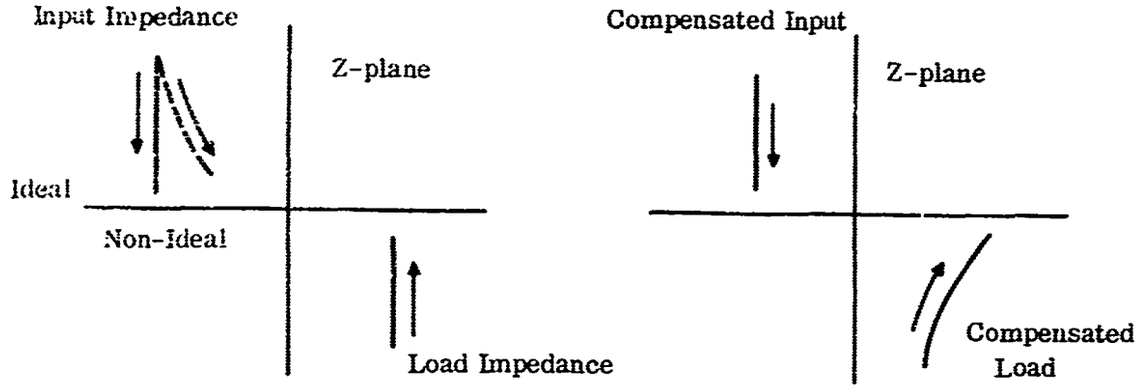

FIG. 4-5: Effect of Lcad Compensation.

lies entirely in the right-half Z-plane, it is reasonable to suppose that it could be realized with passive elements. An attempt to apply this same technique to the LC realization would lead, in general, to a compensated load-impedance locus which crossed the Im-axis of the Z-plane and which would, therefore, be unrealizable with passive elements.

Another realization is obtained by expanding the negative term in Eq. (4.17) in the form

$$-\frac{as}{(s+a)(1-a^2)} = -\frac{a}{1-a^2} + \frac{a^2}{(s+a)(1-a^2)} \qquad (4.20)$$

which has the form of an RL admittance in parallel with a negative conductance. This expansion leads to the realization shown in Fig. 4-6. Since the use of inductance is generally undesirable and since it is generally somewhat more

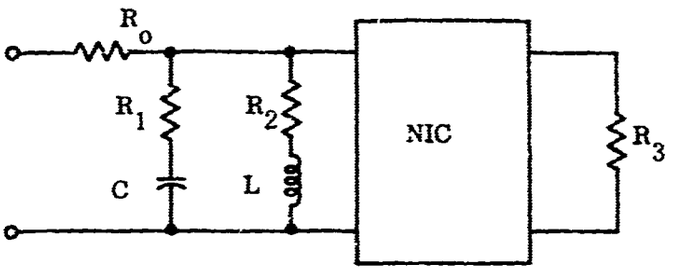

with

$$R_0 = \frac{1+a^2}{a} \qquad R_1 = \frac{1-a^2}{a} \qquad R_2 = \frac{1-a^2}{a} \qquad R_3 = \frac{1-a^2}{a}$$

$$C = \frac{a^2}{1-a^2} \qquad L = \frac{1-a^2}{a^2}$$

FIG. 4-6: Negative R Realization.

difficult to compensate for NIC imperfections with a constant load, as opposed to a load which is a function of frequency, the realization of Fig. 4-6 is not as useful as those of Figs. 4-3 and 4-4.

4.6 NIC Circuits

A particularly simple NIC circuit is given in Fig. 4-7a. It is easily seen

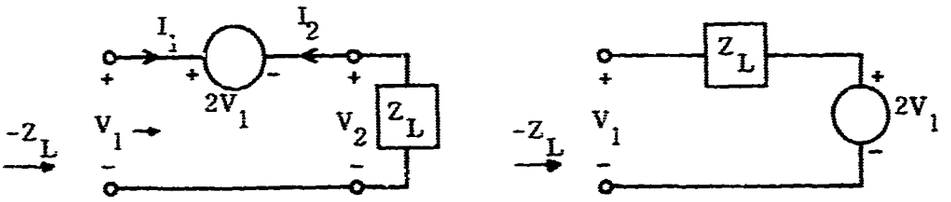

FIG. 4-7: Voltage Amplifier NIC.

that $V_2 = -V_1$; therefore

$$I_2 = -V_2/Z_L = V_1/V_L \tag{4.21}$$

and

$$Z_{in} = V_1/I_1 = -V_1/I_2 = -Z_L \ . \tag{4.22}$$

The modified configuration of Fig. 4-7b yields the same result and is somewhat easier to achieve in practice; this configuration is not a true two-port NIC, but it is usable in the one-port application being considered here.

A non-inverting amplifier with a gain of 2 can be constructed using two high-gain inverting amplifiers with negative feedback around each stage to give a stage gain of $\sqrt{2}$, as shown in Fig. 4-8. Assuming that each amplifier has input

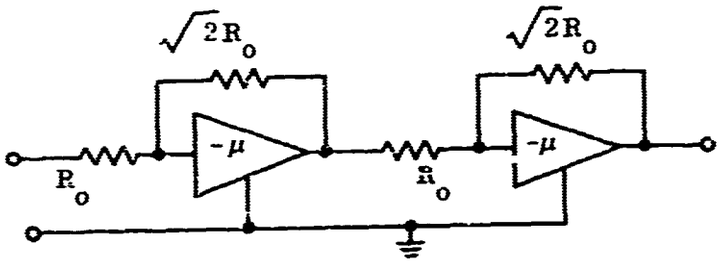

FIG. 4-8: Non-Inverting Amplifier.

and output impedances equal to R_0, and connecting a load admittance Y between the input and output terminals, the input impedance is found to be of the form

$$Y_{in} = \frac{a - bY}{c + dY} \tag{4.23}$$

where a, b, c, and d are positive constants. Letting

$$Y = \frac{a}{b} + Y_L \tag{4.24}$$

which is equivalent to adding a shunt conductance $G_2 = a/b$. yields

$$Z_{in} = \frac{c + \frac{ad}{b} + dY_L}{-bY_L} \quad . \tag{4.25}$$

Finally, adding a series resistance

$$R_i = d/b \tag{4.26}$$

gives

$$Z_{in} = -\frac{ad + bc}{b^2} Z_L \quad . \tag{4.27}$$

This circuit was constructed using RCA CA 3004 wideband amplifiers as the active elements. Without the load, the circuit operated satisfactorily as a non-inverting amplifier, although it was more sensitive to variations in supply voltage than might have been anticipated. When the load was added, the sensitivity became extremely critical; the range of supply voltage over which the circuit exhibited NIC action was only a few tenths of a volt, and there was a very strong tendency toward high-frequency oscillation. Further development of the circuit was therefore discontinued.

Another NIC realization uses a differential-input, operational amplifier, as shown in Fig. 4-9. Assuming that the amplifier has high gain and infinite input

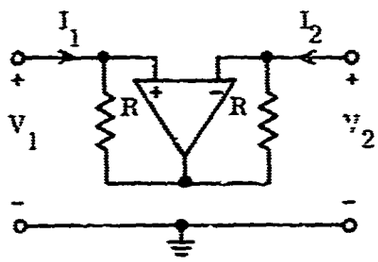

FIG. 4-9: Operational Amplifier NIC.

impedance, there is a virtual short at the input terminals, which implies that $V_1 = V_2$. The two resistors thus have equal voltages across them, and since the amplifier draws no input current we have $I_1 = I_2$, satisfying the conditions for NIC operation.

For low-frequency operation, this circuit is quite attractive, since suitable operational amplifiers are readily available in integrated form. However, a number of undesirable effects are observed as frequency is increased. The input impedance can no longer be assumed to be infinite, due to the presence of shunt capacitance. The impedance between the two input terminals does not seriously degrade performance, since the inputs are at approximately equal potentials. The impedance between each input and ground cancel one another by NIC action provided that the circuit operates as a perfect NIC with unit conversion ratio.

Another high-frequency effect is the variation of amplifier gain in both magnitude and phase. The latter is the more important factor since in general phase-shift becomes appreciable at frequencies a decade below the 3 dB point. In order to maintain stability and minimize noise, commercially available operational amplifiers generally have a controlled gain roll-off at a relatively low frequency, making them unsuitable for the proposed application at frequencies much in excess of 1 MHz.

In order to be able to more readily make circuit modifications, a breadboard amplifier was constructed using a conventional differential input stage driving a common-emitter stage. A variety of compensation schemes were tried, using frequency-dependent coupling and/or feedback networks, etc., in an attempt to achieve zero phase-shift along with reasonably flat gain. Although this goal was realized, the cost in gain reduction was prohibitive; the compensation reduced the gain to less than 10 dB. Additional stages to increase gain also introduced undesirable phase shift. It was concluded that the operational amplifier NIC was not suitable for high-frequency operation. This conclusion is subject to modification by state-of-the-art developments in operational amplifier technology, although it is difficult to be optimistic about the possibility of obtaining high gain, zero phase-shift, and high input impedance in the VHF range.

4.7 The Yanagisawa NIC

The NIC circuit which gave the best experimental results was described originally by Yanagisawa (1957). The circuit is shown in Fig. 4-10 in simplified

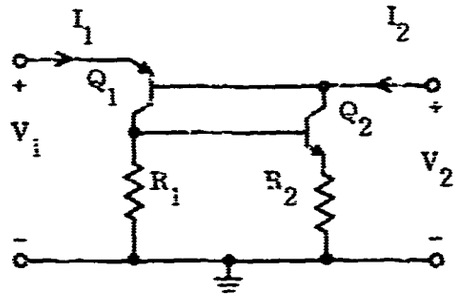

FIG. 4-10: Yanagisawa NIC.

form, with all bias and compensation circuits omitted. Assuming that $V_{BE} = 0$ in both transistors, we have $V_1 = V_2$. Further assuming that $\alpha = 1$, all of I_1 flows through R_1, developing a voltage $R_1 I_1$ which also appears across R_2. The emitter current of Q_2 is therefore $I_1 R_1 / R_2$; since both base currents are assumed zero, this is also the value of I_2. We have, therefore

$$V_i = V_2 \tag{4.28a}$$

$$I_2 = \frac{R_1}{R_2} I_1 \tag{4.28b}$$

which describes a NIC with

$$Z_{in} = -\frac{R_1}{R_2} Z_L \quad . \tag{4.29}$$

In practice, of course, each transistor must have a collector supply circuit; however, if these are identical and the NIC conversion factor is -1, then the collector impedances cancel one another, since one is across the input and the other across the output for AC.

At higher frequencies, the collector capacitances must be considered. As previously reported (McMahon, 1970), a simple analysis yields

$$h_{11} = 0 \qquad h_{12} = 1$$

$$h_{21} = (R_1/R_2)\,\frac{1 - sCR_2}{1 + sCR_1} \qquad h_{22} = sC\,\frac{1 + (R_1/R_2)}{1 + sCR_1} \tag{4.30}$$

where C is the sum of the collector-base capacitances of Q_1 and Q_2. If R_2 is replaced by a parallel RC combination

$$R_2 \rightarrow \frac{R_2}{1 + sC_2R_2} \tag{4.31}$$

with $R_1 = R_2$ and $C_2 = 2C$, we have

$$h_{11} = 0 \qquad h_{12} = 1$$

$$h_{21} = 1 \qquad h_{22} = 2sC \tag{4.32}$$

which describes an ideal NIC except for a parasitic capacitance across the output. In most cases, this capacitance can be absorbed into the load, compensated for at the input, or simply ignored at certain impedance levels and frequencies.

A circuit incorporating this compensation scheme was constructed and tested. The circuit underwent several modifications which, in most cases, were empirical in nature. The results obtained from the final version are discussed in the next Section.

V

EXPERIMENTAL RESULTS

5.1 Measurement Techniques

NIC circuits in general have one open-circuit stable (OCS) port and one short-circuit stable (SCS) port; the device is stable if the impedance loading the OCS port is sufficiently large and that at the SCS port sufficiently small. It was therefore necessary to have two different measurement schemes available to accomodate the loading requirements of the two different orientations.

Fig. 5-1 shows the measurement scheme using a General Radio 1606-A RF Impedance Bridge, which presents a high impedance to the load. The oscilloscope was used to monitor for distortion and possible oscillations, but was removed during the actual measurement.

A low-impedance (50 Ω) measurement scheme using an HP Vector Voltmeter is illustrated in Fig. 5-2. The VVM compares the incident voltage, E_i, at the 50 Ω load with the total voltage, $E_i + E_r$, at the NIC; the quantity actually measured is thus $1+\rho$, which is easily converted to values of Z by use of a Smith Chart or a simple calculation. The system is first calibrated using a short-circuit load in order to compensate for differing line lengths and other sources of undesired phase shift.

The actual NIC circuit and its load are shown in Fig. 5-3. The NIC itself is basically the Yanagisawa circuit of Fig. 4-10 with the addition of biasing. It was found necessary to add the 27K resistor between the two bases in order to obtain reliable turn-on of both transistors; without this resistor, the circuit has a stable state in which both transistors are cut off. To improve stability, the gain is deliberately rolled off at frequencies above 10 MHz by means of the RC circuit in the collector lead of Q_1, while phase-shift is controlled by the emitter of Q_2. The 6.8K resistor at the input and the 10 Ω resistor at the output are for adjustment of impedance levels.

The conversion ratio, Z_{in}/Z_{load} of the NIC was first measured with a 100 Ω load, with the results shown in Table 5.1. As intended, the ratio dropped markedly above 10 MHz, falling to $-.470+j.020$ at 15 MHz.

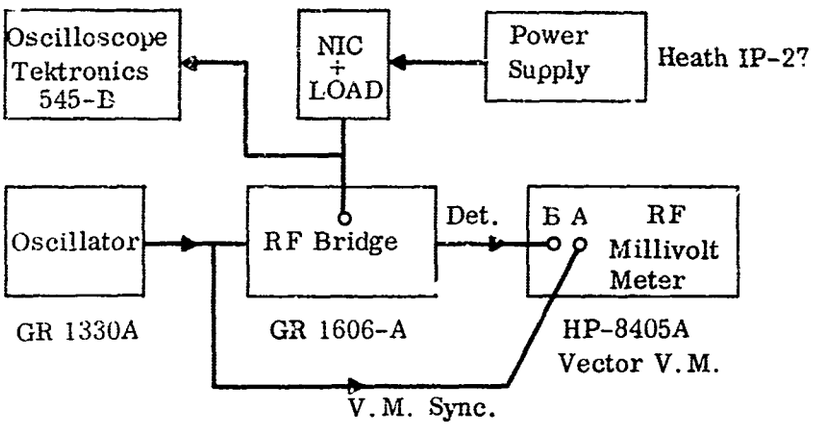

FIG. 5-1: RF Bridge Z Measurement.
(voltmeter null detector)

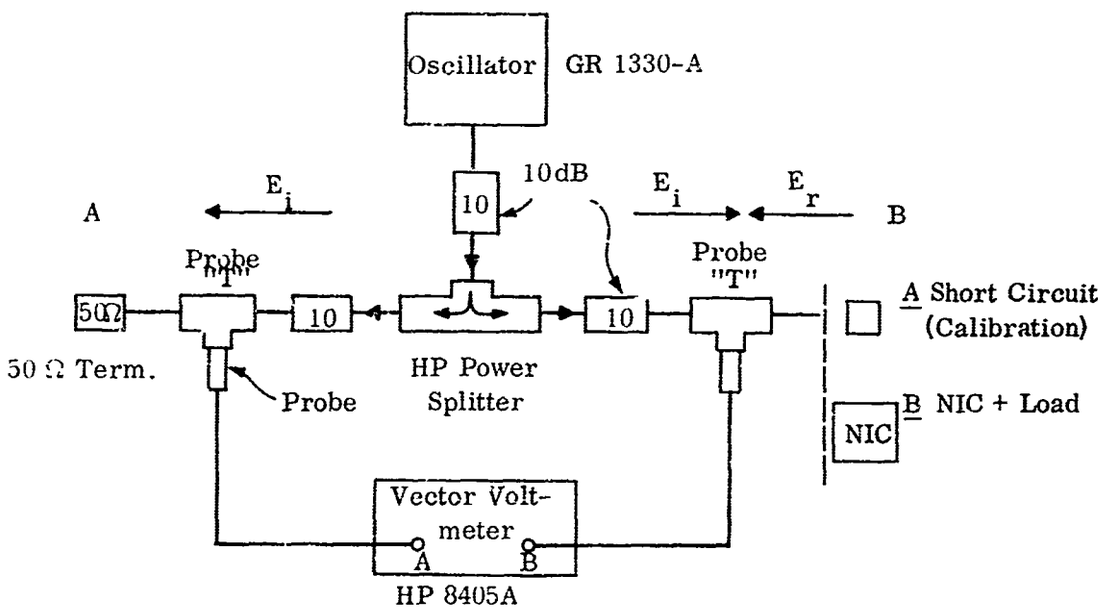

FIG. 5-2: Voltage Reflection Method
of Impedance Measurement.

Note: 1) Voltmeter reads
V_A or V_B and θ_{B-A}

2) $V_A = E_i \angle 0^\circ$

$V_B = (E_i + E_r) \angle \theta^\circ$

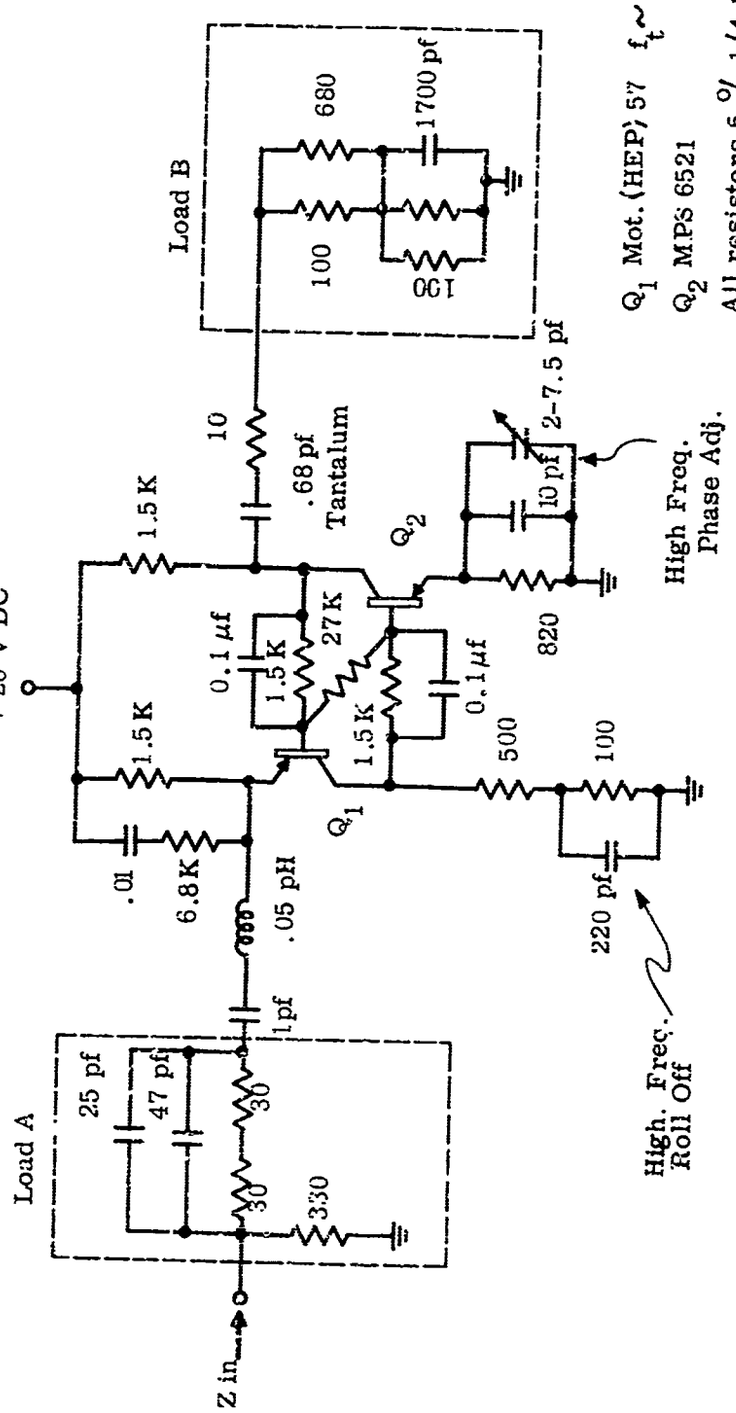

Q_1 Mot. (HEP) 57 $f_t \sim 200$ MHz $\beta \sim 350$

Q_2 MPS 6521

All resistors 5 % 1/4 W, values in ohms

All capacitors 10 % ceramic disk unless noted.

FIG. 5-3: NIC and Loading (1 to 10 MHz).

TABLE 5.1: NIC Conversion Ratio

Frequency MHz	Z_{in}/Z_{load}
1	-.718+j.010
2	-.700+j.025
3	-.685+j.030
4	-.672+j.025
5	-.672+j.018
6	-.667+j.008
7	-.666+j0
8	-.668+j.013
9	-.680+j.028
10	-.700+j.040

Using the measured values of conversion ratio, the element values of the RC realization were scaled to take into account the non-unity conversion ratios. These values were then adjusted experimentally; the only marked variation was in R_1, which should have a value of 59 Ω but which, after adjustment, was 330Ω. This effect has not been satisfactorily explained, but may be due to the interaction of the circuit and the impedance bridge.

Measured values of input impedance, after adjustment, are plotted in Fig. 5-4 and tabulated in Table 5.2. These values were then fitted to a curve of

TABLE 5.2: Measured Values of Input Impedance

f - MHz	R_{in} - Ω	X_{in} - Ω
4	-0.4	11.0
5	0.1	6.2
6	0.2	1.8
7	0.1	-1.9
8	-0.7	-5.5
9	-2.1	-8.1

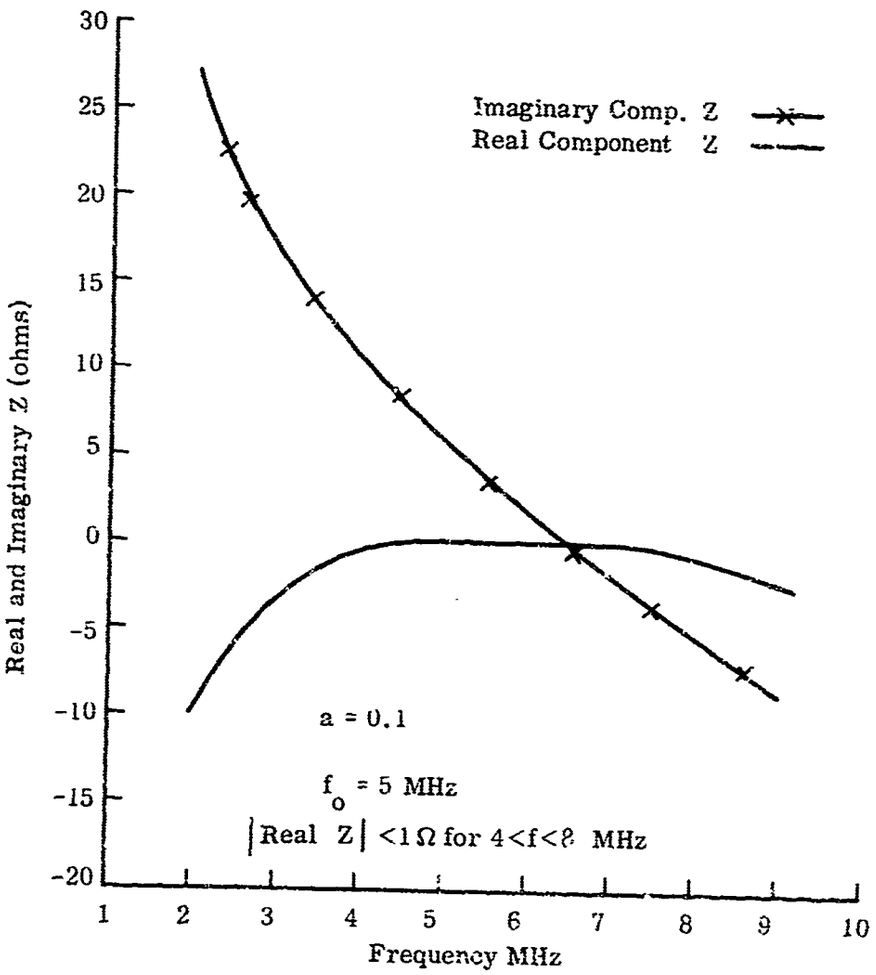

FIG. 5-4: NIC and Load Bridge Measured Impedance.

optimum impedance by choosing a frequency denormalization such that ka = 0.513 at 4 MHz. with a slot width, δ, of 0.09. The cross section reduction was then calculated. with the results given in Table 5.3 and Fig. 5-5.

TABLE 5.3
Calculated Values of Cross Section Reduction

ka	σ/σ_0 - dB
0.513	-14.42
0.642	-18.23
0.770	-19.40
0.898	-23.08
1.027	-6.09
1.155	+2.12

No attempt was made to optimize the fit, on the grounds that the precision of the measurements did not justify such a procedure. Even so, a cross section reduction of 13dB or better was achieved over an approximate 2:1 frequency range from ka = 0.5 tc ka = 1.0. Since no previous experimental results have shown bandwidths of more than a few per cent. this is a significant result which verifies the basic suitability of the NIC realization. Admittedly, the frequency range is lower than that originally aimed for, but this is a result of state-of-the-art limitations on transistors and circuit construction techniques rather than any fundamental limitation of the realization technique itself.

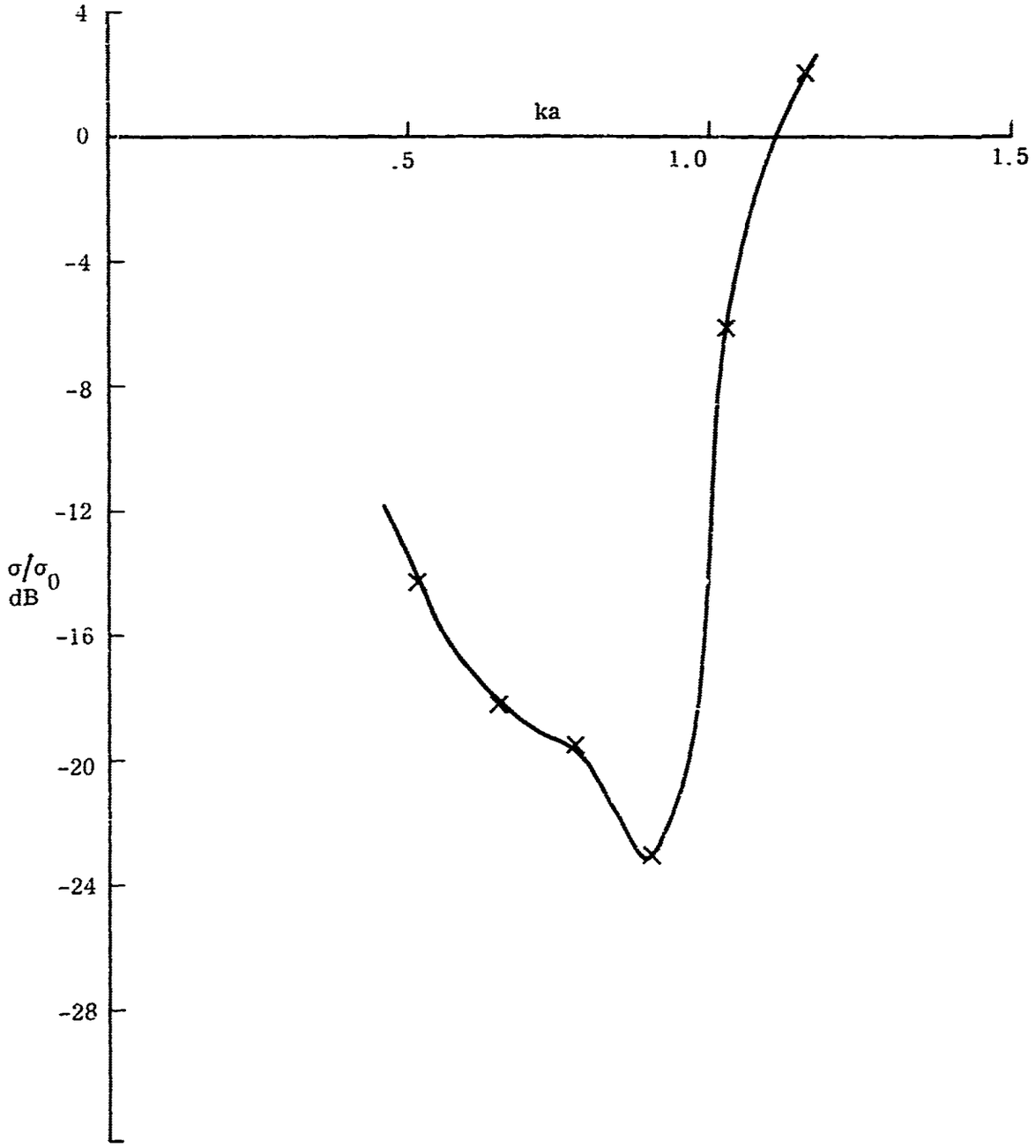

FIG. 5-5: Calculated Cross-Section Reduction for Measured Impedance Values.

VI

PROSPECTS FOR FURTHER DEVELOPMENT

From an evaluation of the results presented in this report, it appears that neither the lumped nor the distributed passive loads would provide the required impedance variation for broadband cross section control. The only alternative is thus the use of active devices, and of these the Yanagisawa NIC circuit could almost certainly be made to operate at higher center frequencies by using transistors with higher f_T's, although stability would very likely present difficulties. In conjunction with more sophisticated circuit techniques (e.g., strip line), an order of magnitude increase in frequency might be achieved. The requirements are stringent, however; a transistor with $\beta = 100$ and $f_T = 2\,GHz$, for example, has a beta-cutoff frequency of 20 MHz and exhibits significant phase shift at 2 MHz. Compensation might make such a transistor usable at frequencies as high as 20 or 30 MHz, but it is obvious that substantial improvement in performance must await major developments in transistor technology: f_T's of 10 GHz or more, with reasonably large β's.

Another possibility would be to develop a circuit which exhibits some degree of NIC action in the desired frequency range, however imperfectly, and then use load compensation to achieve the desired result. Since there is no well-developed theory of synthesis with imperfect active devices, this would be primarily an empirical procedure, with no guarantee that the required load compensation would be realizable. However, this approach would seem to be worth some further consideration.

Integrated-circuit technology could contribute most to this problem through development of a true VHF operational amplifier. The op-amp is one of the commonest linear IC's available, and rapid advances in performance are being made. If a differential-input amplifier with high gain, high input impedance, and low output impedance at VHF should become available, the configuration of Fig. 4-9 should be useful.

Finally, since the necessary amplifiers are presently available in integrated form, the circuit of Fig. 4-8 warrents further study. This circuit has very severe stability problems, but perhaps a way to overcome them might be found.

REFERENCES

Ås, B.O. and H.J. Schmitt (1958) "Back Scattering Cross Section of Reactively Loaded Cylindrical Antennas", Harvard University Cruft Laboratory Scientific Report No. 18.

Chang, S. and T.B.A. Senior (1967) "Study of Scattering Behavior of a Sphere with an Arbitrarily Placed Circumferential Slot". The University of Michigan Radiation Laboratory Report No. 5548-6-T.

Chen, K-M (1965) "The Minimization of Back Scattering of a Cylinder by Double Loading". The University of Michigan Radiation Laboratory Report No. 5548-4-T.

Chen, K-M (1968) "Minimization of Radar Cross Sections of Cylinders by Compensation Method". Scientific Report No 1, Division of Engineering Research, Michigan State University.

Chen, K-M and V.V. Liepa (1964) "The Minimization of the Radar Cross Section of a Cylinder by Central Loading". The University of Michigan Radiation Laboratory Report No. 5548-1-T.

Hu Y-Y (1958) "Backscattering Cross Section of a Center-Loaded Cylindrical Antenna". IRE Trans. AP-6. 140-148.

Iams, H.A. (1950) "Radio Wave Conducting Device", U.S. Patent No. 2,578,367.

King, R.W.P. (1956) The Theory of Linear Antennas. Harvard University Press. Cambridge. Massachusetts.

McMahon, E.L. (1969) "Computed Cross Section Reduction for Various Loads". The University of Michigan Radiation Laboratory Internal Memorandum No. 01363-511-M.

McMahon, E.L. (1970) "Circuit Realization of Impedance Loading for Cross Section Reduction". The University of Michigan Radiation Laboratory Report No. 01363-7-T.

McMahon E.L., A.R. Braun and R.S. Kasevich (1968) "Network Theory Problems in Impedance Loading". The University of Michigan Radiation Laboratory Report No. 5548-8-T.

Liepa, V.V. and T.B.A. Senior (1964) "Modification to the Scattering Behavior of a Sphere by Reactive Loading". The University of Michigan Radiation Laboratory Report No. 5548-2-T.

Liepa, V.V. and T B.A. Senior (1966) "Theoretical and Experimental Study of the Scattering Behavior of a Circumferentially Loaded Sphere". The University of Michigan Radiation Laboratory Report No. 5548-5-T.

Senior, T.B.A. and E.F. Knott (1967a) "Research on Resonant Region Radar Camouflage Techniques - Third Interim". The University of Michigan Radiation Laboratory Report No. 8077-3-T, AD 380204. SECRET.

Senior, T.B.A. and E.F. Knott (1967b) "Research on Resonant Region Radar Camouflage Techniques - Fourth Interim", The University of Michigan Radiation Laboratory Report No. 8077-5-T, AD 382138. SECRET.

Ramo, S. and J.R. Whinnery (1958) Fields and Waves in Modern Radio, John Wiley and Sons, Inc., New York, Second Edition.

Sletten, C.J., P. Blacksmith, F. S. Holt and B.B.Gorr (1962) "Reduction of Radar Scatter from Resonant Objects by Reactive Loading", Air Force Cambridge Research Laboratories Report AFCRL 62-754.

Smit, J. and H.P.J. Wijn (1969) Ferrites, John Wiley and Sons, Inc., New York.

Vincent, M.C. and K-M Chen (1968) "Experimental Investigation of the Modification of the Backscattering Cross Section of Metallic Objects", Scientific Report No. 5, Division of Engineering Research, Michigan State University.

Yanagisawa, T. (1957) "RC Active Networks Using Current Inversion Type Negative-Impedance Converters", IRE Trans. CT-4, 124-131.